THE JOURNAL OF BIOLOGICAL CHEMISTRY VOL. 283, NO. 44, pp. 30034–30044, October 31, 2008

Nck Adapters Are Involved in the Formation of Dorsal Ruffles, Cell Migration, and Rho Signaling Downstream of the Platelet-derived Growth Factor β Receptor*[S]

Received for publication, February 4, 2008, and in revised form, July 9, 2008 Published, JBC Papers in Press, September 2, 2008, DOI 10.1074/jbc.M800913200

Aino Ruusala[‡], Tony Pawson[§], Carl-Henrik Heldin[‡], and Pontus Aspenström[‡¶1]

From the [‡]Ludwig Institute for Cancer Research, Biomedical Center, Uppsala University, SE-751 24 Uppsala, Sweden, the [§]Samuel Lunenfeld Research Institute, Mount Sinai Hospital, Toronto, Ontario M5G 1X5, Canada, and the [¶]Department of Microbiology, Tumour and Cell Biology, Karolinska Institute, SE-171 77 Stockholm, Sweden

The SH3 and SH2 domain-containing adapter proteins Nck1 and Nck2 are known to function downstream of activated tyrosine kinase receptors, such as the platelet-derived growth factor (PDGF) receptors. The SH2 domain of Nck1 binds to phosphorylated tyrosine residue 751 in PDGFβ receptor and has been suggested to have a role in the PDGF-induced mobilization of the actin filament system. Because Tyr-751 is a site for additional receptor interactors, it has been difficult to discriminate the signaling from Nck from signaling via other molecules. For this reason we have used mouse embryonic fibroblasts derived from mice in which the genes for Nck1 and Nck2 have been inactivated by gene targeting (knock-out (KO) cells). The mutant cells had a reduced ability to form edge ruffles in response to PDGF, and the presence of Nck was obligatory for the formation of dorsal ruffles. In addition, the KO cells had a reduced chemotactic and migratory potential. Importantly, KO cells had reduced cell attachment properties and a reduced ability to form focal adhesions in response to serum stimulation. Moreover, signaling involving the Rho GTPases was defective in KO cells. In summary, our observations suggest that the Nck adapters are needed for signaling to Rho GTPases and actin dynamics downstream of the PDGFβ receptor.

There is a close correlation between the activities of tyrosine kinase receptors and the dynamic reorganization of the actin filament system (1, 2). Tyrosine kinase receptors, such as the platelet-derived growth factor (PDGF)[2] β receptor (PDGFRβ), exert their action by ligand-induced receptor dimerization, which induces transphosphorylation of the two receptor molecules. The phosphorylated tyrosine residues in the activated PDGF receptor constitute docking sites for SH2 domain-containing proteins (1, 2). The role of the individual tyrosine residues in PDGF signaling has been extensively studied in cells such as fibroblasts and porcine aortic endothelial (PAE) cells expressing mutant PDGFRβ in which specific tyrosine residues in the cytoplasmic part of the PDGFRβ have been replaced with phenylalanine residues (1, 2). Using this approach, the specific importance of individual tyrosine residues for binding and activation of downstream signaling proteins has been studied. PDGFRβ-mediated mobilization of the actin filament system, seen as the formation of membrane ruffles, has been found to require the activity of the phosphoinositide 3-kinase (PI3K)/Rac signaling pathway (3–5). PDGFRβ with mutated tyrosine residues 740 and 751 (PDGFRβ-Y740F/Y751F) can no longer bind the SH2 domain of the p85 regulatory subunit of PI3K (6). Moreover, the PDGFRβ-Y740F/Y751F-expressing PAE cells do not form membrane ruffles in response to PDGF-BB (3, 4). Several of the phosphotyrosines in activated PDGFRβ constitute docking sites for multiple substrates, *i.e.* the tyrosine residue 751 is also the docking site for Nck1, and the phospholipase Cγ- and SHP2-binding site tyrosine 1009 is also a binding site for Nck2 (7–12). Hence, studies of cell lines harboring mutant PDGFRβ receptors will not discriminate between the different potential binding partners for the receptor.

The Nck family of adapter proteins consists of two gene products, Nck1 and Nck2 (13, 14). Nck was shown to be a substrate for tyrosine kinase receptors and to have tumor promoting activities (15, 16). Nck adaptors have also been implicated in the regulation of the actin filament system (for review, see Refs. 17 and 18). Many proteins that directly influence the actin polymerization machinery, such as Wiskott-Aldrich syndrome protein (WASP), WASP-interacting protein, and p21-activated kinase (Pak), can directly bind to the SH3 domains of Nck (for review, see Ref. 17). Most studies on the Nck adaptors have so far been focused on Nck1, and it is not known to what extent there exists a functional redundancy between the two paralogues. It is somewhat surprising that Nck1 and Nck2 seem to have separate binding sites on the activated PDGFRβ as the SH2 domains of the two adapters are almost identical. In an effort to study the involvement of the Nck adaptor proteins in PDGF signaling separate from PI3K-mediated signaling, we used mouse embryonic fibroblasts (MEFs) in which the Nck1 and Nck2 genes had been inactivated by gene targeting (KO cells) (19).

* This work was supported in part by grants from the Swedish Cancer Society and the Swedish Research Council. The costs of publication of this article were defrayed in part by the payment of page charges. This article must therefore be hereby marked "*advertisement*" in accordance with 18 U.S.C. Section 1734 solely to indicate this fact.

[S] The on-line version of this article (available at http://www.jbc.org) contains supplemental Figs. 1–3.

[1] To whom correspondence should be addressed. Tel.: 46-8-524-87-188; Fax: 46-8-330498; E-mail: pontus.aspenstrom@ki.se.

[2] The abbreviations used are: PDGF, platelet-derived growth factor; PDGFRβ, PDGFβ receptor; FBS, fetal bovine serum; GST, glutathione *S*-transferase; KO, knock out; MEF, mouse embryonic fibroblast, PAE, porcine aortic endothelial; PI3K, phosphoinositide 3-kinase; TRITC, tetramethylrhodamine isothiocyanate; WASP, Wiskott-Aldrich syndrome protein; WT, wild type; siRNA, small interfering RNA; PBS, phosphate-buffered saline.

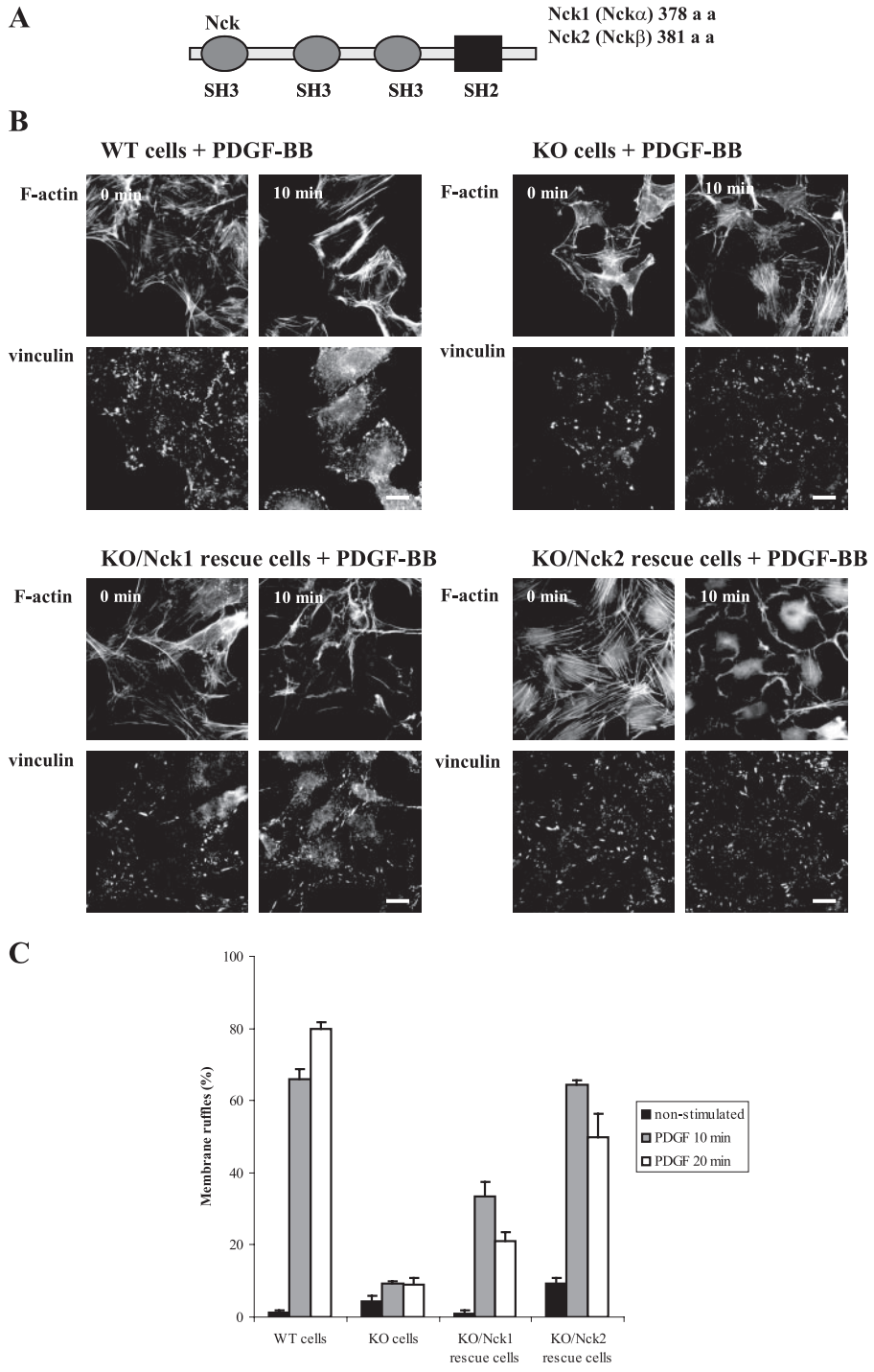

FIGURE 1. **Nck adapters are required for membrane ruffling induced by PDGF-BB.** *A*, schematic representation of Nck1 and Nck2. *B*, WT, KO, KO/Nck1 rescue, and KO/Nck2 rescue cells were stimulated with 100 ng/ml of PDGF-BB for 10 min. Filamentous actin was detected by fluorescein isothiocyanate-conjugated phalloidin. Vinculin was detected by a mouse anti-vinculin antibody followed by a TRITC-conjugated anti-mouse antibody. The *bar* represents 20 μm. *C*, quantification of the PDGF-induced membrane ruffling activity after 10 and 20 min was performed by microscopy analysis. The values represent analyses of at least 100 cells from 3 independent experiments.

EXPERIMENTAL PROCEDURES

Antibodies and Plasmids—Rabbit polyclonal anti-Arp3A antiserum was a generous gift from L. Machesky, Birmingham, UK. Rabbit polyclonal anti-N-WASP antiserum was raised against a peptide, CRFYGPQVNNISHTKEKK, which represents amino acid residues 173–189 of the human N-WASP. In addition, the following antibodies were used: mouse monoclonal anti-Myc (Santa Cruz Biotechnology), mouse monoclonal anti-RhoA (Santa Cruz), anti-phosphotyrosine (PY99, Santa Cruz), mouse monoclonal anti-vinculin and mouse monoclonal anti-α-tubulin (Sigma), mouse monoclonal anti-Rac1 (Upstate Biotechnology, Inc.), mouse monoclonal anti-Nck (BD Transduction Laboratories), rabbit anti-phospho-Akt (serine 473, Cell Signaling Technology), rabbit anti-Akt (Cell Signaling Technology), AlexaFluor 488-conjugated anti-mouse antibodies (Molecular Probes), TRITC-conjugated anti-mouse (Jackson ImmunoResearch Laboratories), and TRITC-conjugated anti-rabbit (DAKO). TRITC-labeled phalloidin, fluorescein isothiocyanate-labeled phalloidin (Sigma), or AlexaFluor 488-conjugated phalloidin (Molecular Probes) were used to visualize filamentous actin. The vectors expressing the constitutively active Rho GTPases have been described before (20).

Cell Cultivation—The establishment of MEFs from Nck1/2$^{-/-}$ mice has been shown in a previous article (19). Wild-type, Nck1/2$^{-/-}$, and Nck1/2$^{-/-}$ cells in which Nck1 had been stably transfected (in this article called WT, KO, and KO/Nck1 rescue cells, respectively) were cultured in Dulbecco's modified Eagle's medium supplemented with 10% FBS. KO/Nck2 rescue cells were created by stably expressing mouse Nck2 in KO MEFs essentially as described before (19). Porcine aortic endothelial (PAE) cells stably transfected with the human PDGFβ receptor, harboring point mutations in tyrosine residues 740 or 751, PAE/PDGFRβ-Y740 or PAE/PDGFRβ-Y751 mutant receptor-expressing cells, were cultured in Ham's F-12 medium supplemented with 10% FBS. The cells were cultured at 37 °C in an atmosphere of 5% CO_2. Knock-down of Nck expression was triggered by transfection of WT MEFs with double-stranded Nck1- or Nck2-specific small interfering RNA (siRNA) (Sigma) or a control siRNA employing the Silentfect transfection reagent and protocol (Bio-Rad). For immunostaining purposes, cells were seeded on coverslips and trans-

fected by Lipofectamine according to the procedure provided by the manufacturer. For cell staining, the cells on the coverslips were fixed in 2% paraformaldehyde in PBS for 20 min at room temperature. The cells were permeabilized in 0.5% Triton X-100 in PBS for 5 min and thereafter washed again and incubated in the presence of 0.01 M glycine in PBS for 1 h. The slides prepared for visualization of endogenous N-WASP and Arp3A were instead fixed in ice-cold methanol for 10 min and blocked in 0.01 M glycine, PBS for 1 h. Primary and secondary antibodies were diluted in PBS containing 5% FBS. Cells were incubated with primary antibodies followed by secondary antibodies for intervals of 1 h. The coverslips were mounted on object slides in Fluoromount-G mounting medium (Southern Biotechnology Associates). The cells were photographed by a Hamamatsu ORCA CCD digital camera employing the QED Imaging System software using a Zeiss Axioplan2 microscope.

For Western blotting analysis, cell lysis was performed essentially as described before (20). The cell lysates were subjected to SDS-PAGE, and the proteins were then transferred to Hybond-C Extra nitrocellulose filters (GE Healthcare). Western blotting was performed with primary mouse or rabbit antibodies followed by horseradish peroxide-conjugated anti-mouse or anti-rabbit secondary antibodies (GE Healthcare). The Western blots were detected by the Luminol Western blotting substrate (Santa Cruz).

Chemotaxis Analysis—A detailed description of the assay has been described before (21). Briefly, chemotaxis was measured using the ChemoTx System 96-well disposable element (Neuro Probe Inc.), 8-μm pore size and 30-μl wells. The wells were coated with 50 μg/ml fibronectin before use. The cells were starved overnight, trypsinized, and washed in the presence of 1% aprotinin. The chemoattractants in starvation medium were added to the lower wells, and the starved cells (50,000 cells per well) were seeded on the upper side of the filter in starvation medium. The chamber was incubated at 37 °C for 4 h, and the cells were fixed to the filter in 96% ethanol, washed in water, and stained with Giemsa solution. The non-migrating cells were removed from the upper site of the filter, and the filter was scanned in a CCD camera (Fuji). Quantifications were performed using Aida Image Analyzer software.

Cell Adhesion Assay—The procedure essentially followed the procedure by Wennerberg *et al.* (22). Briefly, wells in a 96-well microtiter plate were coated with human plasma fibronectin (30 μg/ml), 15% FBS or 1% bovine serum albumin (BSA) at 37 °C for 1 h and blocked with 1% BSA at 37 °C for 1 h. Cells in a serum-free medium were seeded and incubated for 1 h at 37 °C. After washing the wells once with PBS, the attached cells were fixed for 10 min in 96% ethanol at room-temperature, stained with crystal violet for 30 min, washed, and lysed in 1% Triton X-100 for 20 min on a shaker. Bound dye was quantified by measuring the absorbance in the enzyme-linked immunosorbent assay reader at 595 nm.

Protein Production and Rho Activation Assay—Glutathione *S*-transferase (GST) fusion proteins were expressed in *Escherichia coli* and purified on glutathione-Sepharose beads (GE Healthcare). Briefly, the bacteria were lysed in a buffer containing 50 mM Tris-HCl, pH 7.5, 5 mM $MgCl_2$, 50 mM NaCl, 1 mM phenylmethylsulfonyl fluoride, 1% aprotinin (Trasylol, Beyer), and 1 mM dithiothreitol. Activity assays for activated, GTP-bound, Cdc42, Rac1, and RhoA were performed essentially as described before (23).

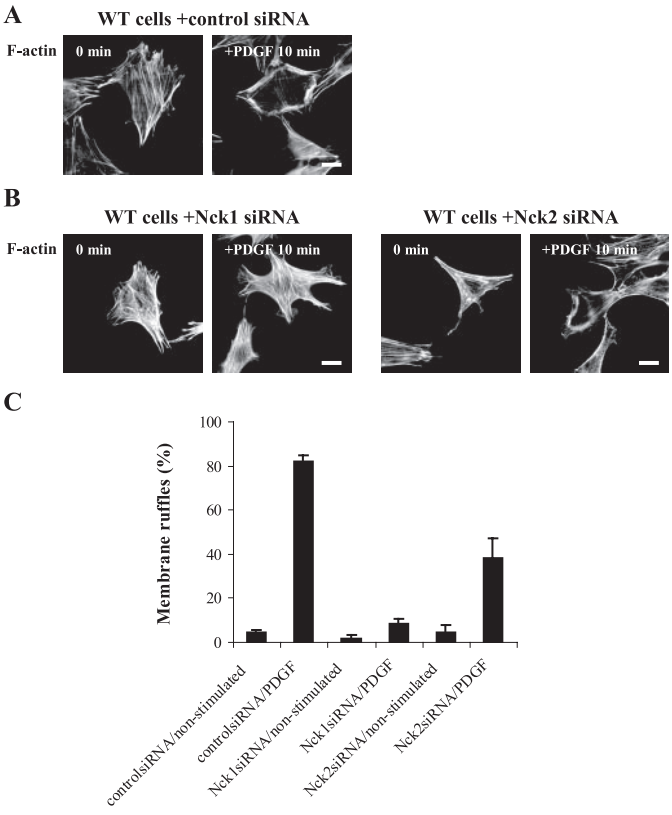

FIGURE 2. **Knock-down of Nck adapters affect the formation of membrane ruffles.** *A*, WT cells transfected with control siRNA were stimulated with 100 ng/ml PDGF-BB for 10 min, and the actin filament system was visualized with AlexaFluor 488-conjugated phalloidin. The *bar* represents 20 μm. *B*, WT cells transfected with siRNA specific for Nck1 or Nck2 were stimulated with 100 ng/ml PDGF-BB for 10 min, and the actin filament system was visualized as in *A*. *Bar* represents 20 μm. *C*, quantification of the membrane ruffling activity was performed by microscopy analysis. The values represent analyses of at least 100 cells from three independent experiments.

RESULTS

Nck Adapters Are Needed for the Formation of Membrane Ruffles—The two members of the Nck family of tyrosine kinase receptor substrates, Nck1 and Nck2, share the same overall primary structure; each of them has three SH3 domains followed by one SH2 domain (Fig. 1*A*). To study the need for Nck in PDGF-induced cytoskeletal reorganization, we used MEFs derived from mice in which *Nck1* and *Nck2* were ablated (KO cells) (19). We first stimulated MEFs isolated from wild-type mice (WT cells) with PDGF-BB for the time periods depicted in Fig. 1*B*. Non-stimulated cells appeared spread, with well developed stress fibers. Visualization of the focal adhesions with an antibody specific for the focal adhesion component vinculin detected the presence of arrowhead-shaped focal adhesions in the non-stimulated cells (Fig. 1, *B* and *C*). PDGF-BB stimulation resulted in a rapid dissolution of the stress fibers and focal adhesions associated with a relocalization of filamentous actin into edge ruffles and dorsal ruffles (also known as circular ruffles). We found that the WT cells had rather small edge ruffles, and but the dorsal ruffles were prominent. After

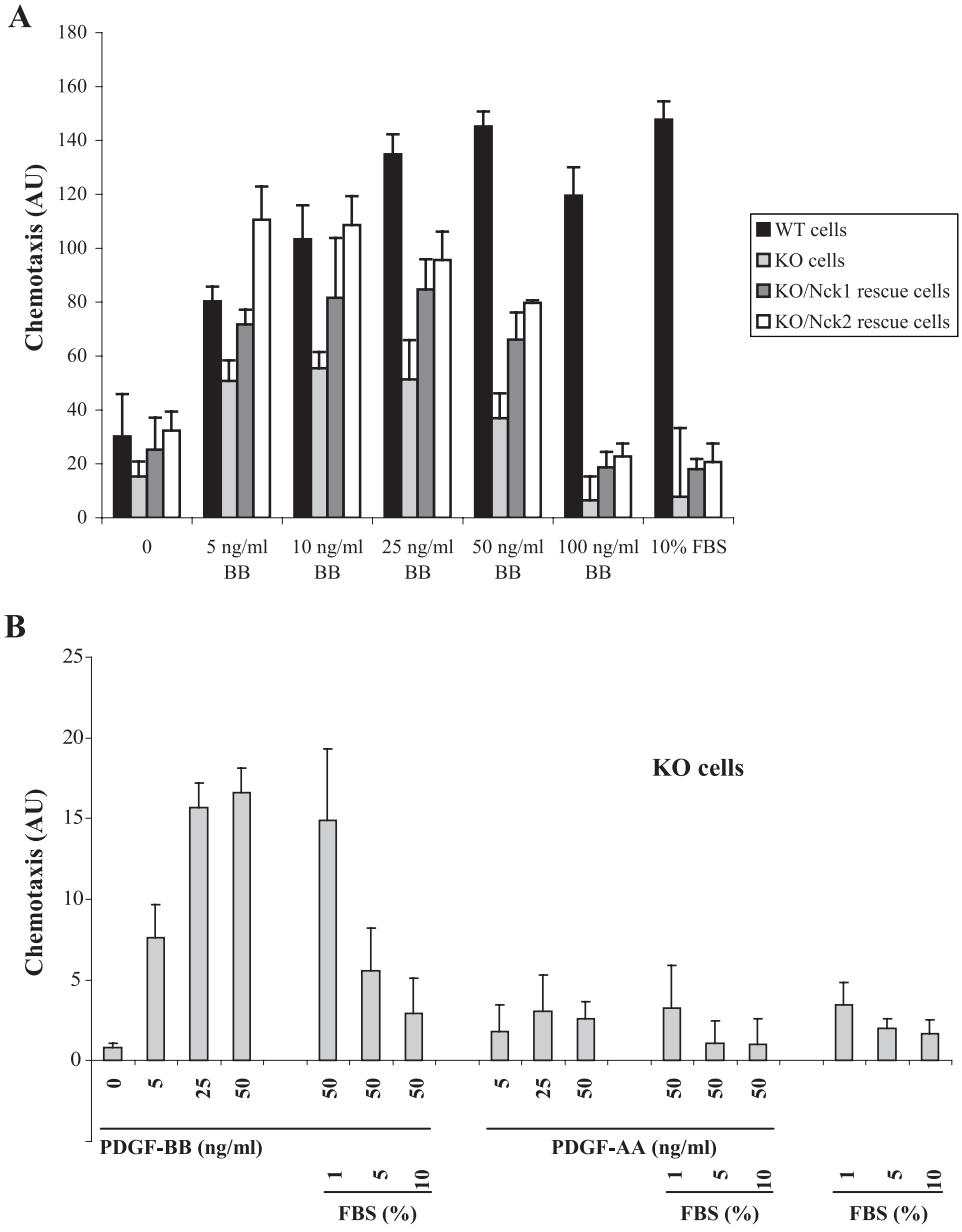

FIGURE 3. **KO cells have a reduced chemotactic ability.** *A*, WT, KO, KO/Nck1 rescue, or KO/Nck2 rescue cells were seeded into filter chambers of the Boyden type. Chemotaxis was triggered by the addition of different amounts of PDGF-BB or 10% FBS. The reaction was terminated after 4 h, and the amount of cells that had passed across the membrane from the upper to the lower phase of the filter was determined in a plate-reader. *B*, KO cells were seeded into filter chambers of the Boyden type. Chemotaxis was triggered by the addition of various combinations of PDGF-BB, PDGF-AA, or FBS as depicted in the figure. The reaction was terminated after 4 h, and the amount of cells that had passed across the membrane from the upper to the lower phase of the filter was determined. Note that the arbitrary units (*AU*) can vary between different experiments due to differences in the color reaction induced by the incubation with Giemsa solution. Therefore, we took care to set up all conditions to be studied on the same filter to allow a true comparison of the chemotactic abilities in the different conditions. This kind of difference are normally avoided by normalizing the chemotactic against the migration in 10% FBS. This could not be done in the present study, as serum strongly interfered with the chemotaxis of the KO and rescue cell lines.

10 min of PDGF-BB stimulation, 66% of the cells and after 20 min 80% of the WT cells had developed dorsal ruffles (Fig. 1, *B* and *C*). Interestingly, the KO cells behaved in a markedly different manner. The cells were smaller than the wild-type MEFs, and PDGF-BB stimulation did not result in any prominent formation of membrane ruffles, and only 9% of the cells displayed some sort of ruffling activity (Fig. 1, *B* and *C*). We also tested KO cells in which the *Nck1* or *Nck2* genes had been reintroduced (KO/Nck1 and KO/Nck2 rescue cells; supplemental Fig. 1*A*). These cells were also smaller than the wild-type MEFs, but in contrast to the KO cells, the PDGF-induced ruffling activity in the KO/Nck1 and KO/Nck2 rescue cells was partially recovered. The KO/Nck2 rescue cells displayed an almost normal membrane ruffling activity. However, the ruffles appeared to be present predominantly at the cell edges rather than on the dorsal side of the cells (Fig. 1, *B* and *C*). The ruffling activity was more transient than in the WT cells, and there was a clear drop in ruffling activity after 20 min of PDGF-BB stimulation in the rescue cell lines.

To confirm the need for Nck adapters in the formation of membrane ruffles, we next treated WT cells with siRNA specific for Nck1 or Nck2 and stimulated the cells with PDGF-BB (the efficiency of Nck knock down is shown in supplemental Fig. 1*B*). Cells transfected with control siRNA behaved as normal WT MEFs, and 82% of the cells had developed membrane ruffles, predominantly dorsal ruffles, after 10 min of stimulation (Fig. 2, *A* and *C*). In contrast, treatment of the WT MEFs with Nck1-specific siRNA almost completely abolished the PDGF-BB responsiveness, and only 8% of the cells displayed membrane ruffles. The Nck2-specific siRNA was less effective in suppressing the PDGF-BB-induced membrane ruffles, and 38% of the cells formed membrane ruffles. Taken together, these observations suggest that the Nck adapters are critical for the formation of dorsal ruffles. Although the individual Nck adapters can partially rescue the membrane ruffling activity, the presence of both Nck paralogues is needed for a full ruffling response.

Nck Adapters Are Needed for Efficient PDGF-BB-induced Chemotaxis—We next tested the requirement for the Nck adapter proteins for PDGF-induced chemotaxis. To this end, cells were seeded in the upper chamber in the ChemoTx chemotaxis system, and PDGF-BB in concentrations ranging from 0 to 100 ng/ml was added to the lower chamber. This triggered the migration of the cells from the upper part of the filter chamber toward the gradient of growth factor in the lower chamber.

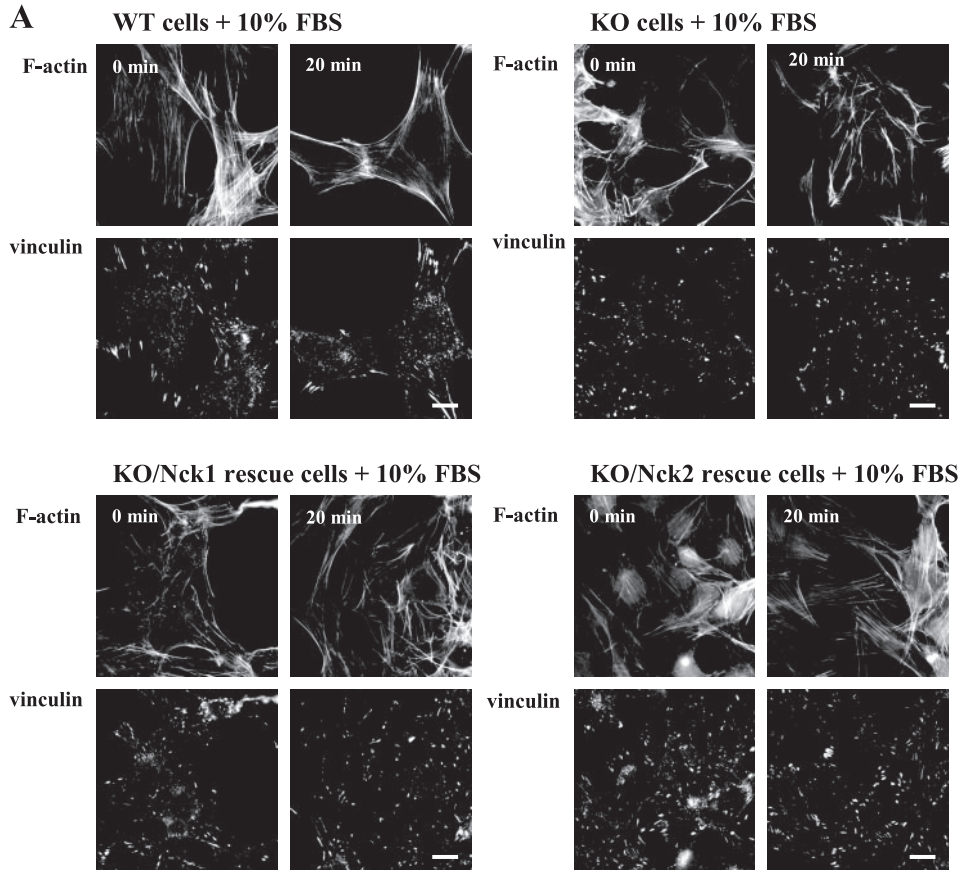

FIGURE 4. **Nck adapters are needed for the assembly of focal adhesions.** *A*, WT, KO, KO/Nck1 rescue and KO/Nck2 rescue cells were serum-starved for 16 h and then stimulated with 10% FBS for different time periods. Filamentous actin was detected by fluorescein isothiocyanate-conjugated phalloidin. Vinculin was detected by a mouse anti-vinculin antibody followed by a TRITC-conjugated anti-mouse antibody. The *bar* represents 20 μm. *B*, quantification of the area of the focal adhesions. Fifteen micrographs of each condition were generated by microscopy analysis. The pictures were taken of randomly chosen areas of the slides. The mean area of the focal adhesions on each micrograph was determined using the ImageJ software and the Analyze Particles function. The statistics analysis was carried out using Student's *t* test. The *, $p < 0.05$; **, $p < 0.01$; ***, represent $p < 0.001$.

The amount of cells that had migrated from the upper to the lower part of the filter after 4 h was determined by a CCD camera, as described under "Experimental Procedures." WT cells migrated efficiently to PDGF-BB; concentrations of PDGF-BB up to 50 ng/ml were increasingly efficient in inducing chemotaxis (Fig. 3*A*). In contrast, KO cells migrated with a reduced efficiency compared with the WT cells (Fig. 3*A*). The KO/Nck1 rescue cells also had a reduced chemotactic response, in particular at higher concentrations of PDGF-BB (Fig. 3*A*). The KO/Nck2 rescue cells displayed a normal migratory ability at lower concentrations of PDGF-BB, but at 25, 50, and 100 mg/ml PDGF-BB they migrated with significantly reduced capacity compared with the WT cells (Fig. 3*A*). We also tested the ability of the WT and KO cells to migrate in a tissue culture wound healing assay. The KO cells had a markedly reduced ability to close the wound compared with wild-type cells (data not shown and Ref. 19). These observations implicate that Nck adapters are needed for an efficient PDGF-BB-dependent chemotaxis; however, the chemotactic response is not entirely ablated by the absence of Nck. Additional signaling pathways, such as the PI3K pathway, are also known to participate in the PDGF-BB-induced chemotaxis. The PI3K/Akt pathway downstream of PDGFRβ is not affected by the genetic inactivation of the Nck adaptors, as PDGF-BB stimulates the phosphorylation of Akt with the same timing and efficiency in WT and KO cells (supplemental Fig. 2*A*). Importantly, PAE cells stably transfected with the PDGFRβY751F had an intact ability to phosphorylate Akt in response to PDGF-BB, whereas the PDGF-BB-dependent Akt phosphorylation was entirely ablated in PAE/PDGFRβ-Y740F mutant cells (supplemental Fig. 2*B*). This is in agreement with the notion that Tyr-740 is the preferred binding site for the p85 subunit of PI3K (although it binds both Tyr-740 and Tyr-751), whereas Nck1 binds only to Tyr-751 (8).

Serum Abolishes Residual PDGF-induced Chemotaxis in Cells Lacking Nck Adapters—Interestingly, although the addition of 10% serum efficiently induced chemotaxis of WT cells, neither the KO, the KO/Nck1 rescue, nor the KO/Nck2 rescue cells moved at all in the presence of 10% FBS (Fig. 3*A*). This was a surprising observation, as FBS normally constitutes an efficient chemotactic cue. We next tested if the inability of the KO cells to move in

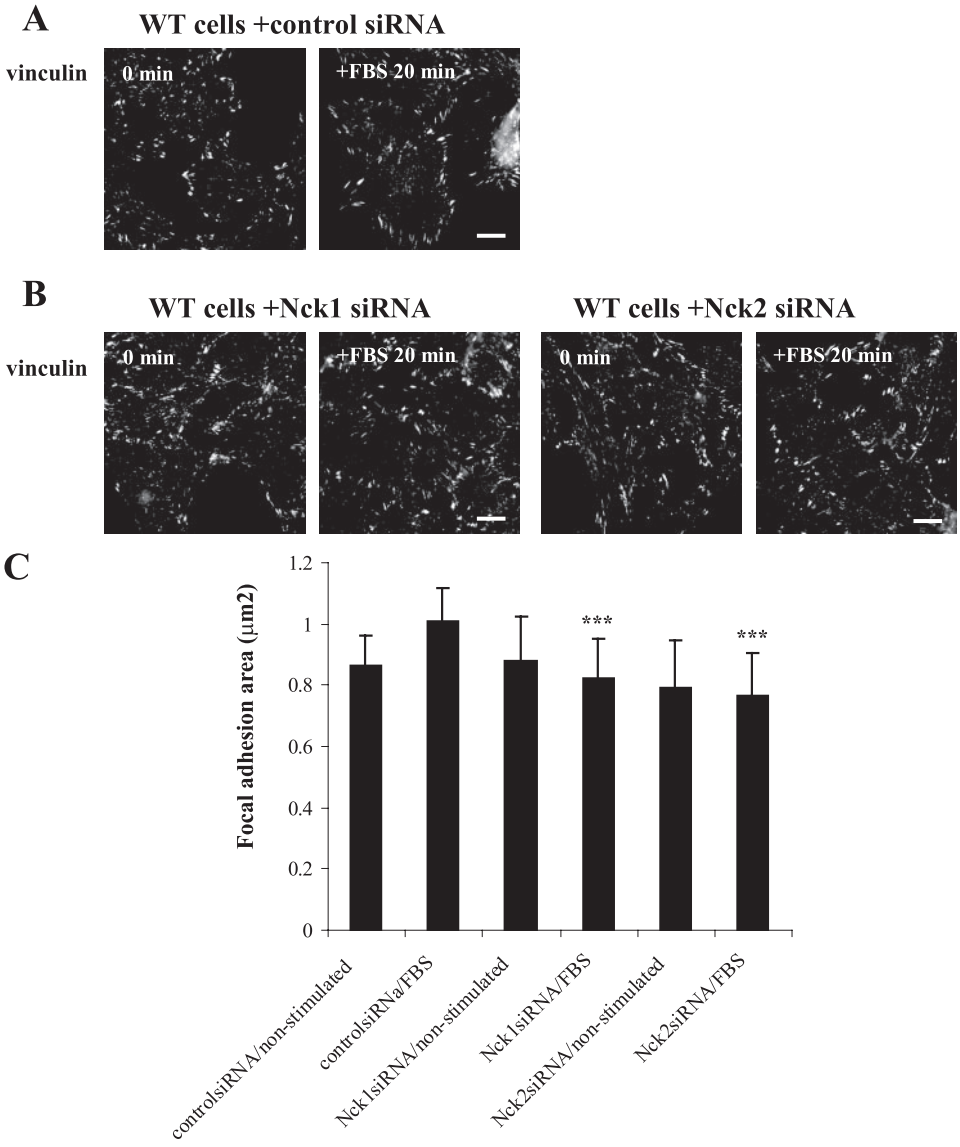

FIGURE 5. **Knock down of Nck adapters decreases focal adhesions.** *A*, WT cells transfected with control siRNA were stimulated with 10% FBS for 20 min, and focal adhesions were visualized by a mouse anti-vinculin antibody followed by a TRITC-conjugated anti-mouse antibody. The *bar* represents 20 μm. *B*, WT cells transfected with siRNA specific for Nck1 or Nck2 were stimulated with 10% FBS for 20 min, and the focal adhesions were visualized as in *A*. The *bar* represents 20 μm. *C*, quantification of the area of the focal adhesions. Fifteen micrographs of each condition were generated by microscopy analysis. The pictures were taken of randomly chosen areas of the slides. The mean area of the focal adhesions on each micrograph was determined using the ImageJ software and the Analyze Particles function. The statistics analysis was carried out using Student's *t* test. *, $p < 0.05$; **, $p < 0.01$; ***, $p < 0.001$.

the presence of serum was caused by an inability of serum constituents to trigger migration of the KO cells or if factors in the serum actively blocked migration. To this end increasing amounts of FBS were added in the presence of 50 ng/ml PDGF-BB. Whereas 1% of serum had a mild effect on the PDGF-BB-induced chemotaxis, 5 and 10% serum efficiently blocked the PDGF-BB-induced migration of the KO cells. PDGF-AA did not induce chemotaxis in the KO cells or in the WT cells, which is consistent with the described inability of the PDGFRα to induce chemotaxis (Fig. 3*B*) (1). No blocking effect of FBS could be seen in WT cells (data not shown). These findings strongly suggest that serum constituents actively block migration of the KO cells.

Cells Lacking Nck Adapters Have a Reduced Ability to Form Focal Adhesions—To gain insights into why the addition of FBS inhibited the chemotactic and migratory properties of the KO cells, we stimulated cells with 10% FBS. The wild-type cells had not entirely lost the stress fibers and focal adhesions upon serum starvation; however, a marked increase in the amount of stress-fibers and focal adhesions could be noticed after 10 min of stimulation, and the size of the focal adhesions increased from 1.4 to 1.9 and 1.8 μm^2 after 10 and 20 min, respectively (Fig. 4, *A* and *B*). In contrast, although the KO cells had some focal adhesions, they were fewer and significantly smaller than in the WT cells (1.1 μm^2), which did increase to 1.3 μm^2 after 20 min, but the size was still significantly smaller than the WT focal adhesions (Fig. 4, *A* and *B*). The response in KO/Nck1 rescue cells very much resembled the one in KO cells with a reduced formation of focal adhesions (Fig. 4, *A* and *B*). In contrast, the focal adhesions in the KO/Nck2 rescue cells were not smaller than the WT cells, but they did not increase in size upon FBS treatment (Fig. 4, *A* and *B*).

To confirm the need for Nck adapters in the formation of focal adhesions, we treated WT cells with siRNA specific for Nck1 or Nck2 and stimulated the cells with 10% FBS for 20 min. The focal adhesions were again visualized with a vinculin-specific antibody, and mean area of the focal adhesions was measured before and after FBS treatment (Fig. 5*A*). In control siRNA-treated cells the mean area increased from 0.9 to 1.0 μm^2, which is a significant increase in the surface area (Fig. 5, *A* and *C*). The apparent size of the focal adhesions are generally smaller under this experimental conditions, as the cells are allowed to attached for shorter periods and are kept in the absence of serum for most of the transfection procedure. The surface area of the focal adhesions in the Nck1- and Nck2-specific siRNA-treated cells were in the same range as in the control siRNA-treated cells (0.9 and 0.8 μm^2, respectively), but importantly, the surface area of the focal adhesions did not increase upon FBS treatment (Fig. 5, *B* and *C*). Taken together, the data suggest that the presence of Nck2 is enough for the restoration of the full size of the focal adhesion but that both adapters are required for a dynamic

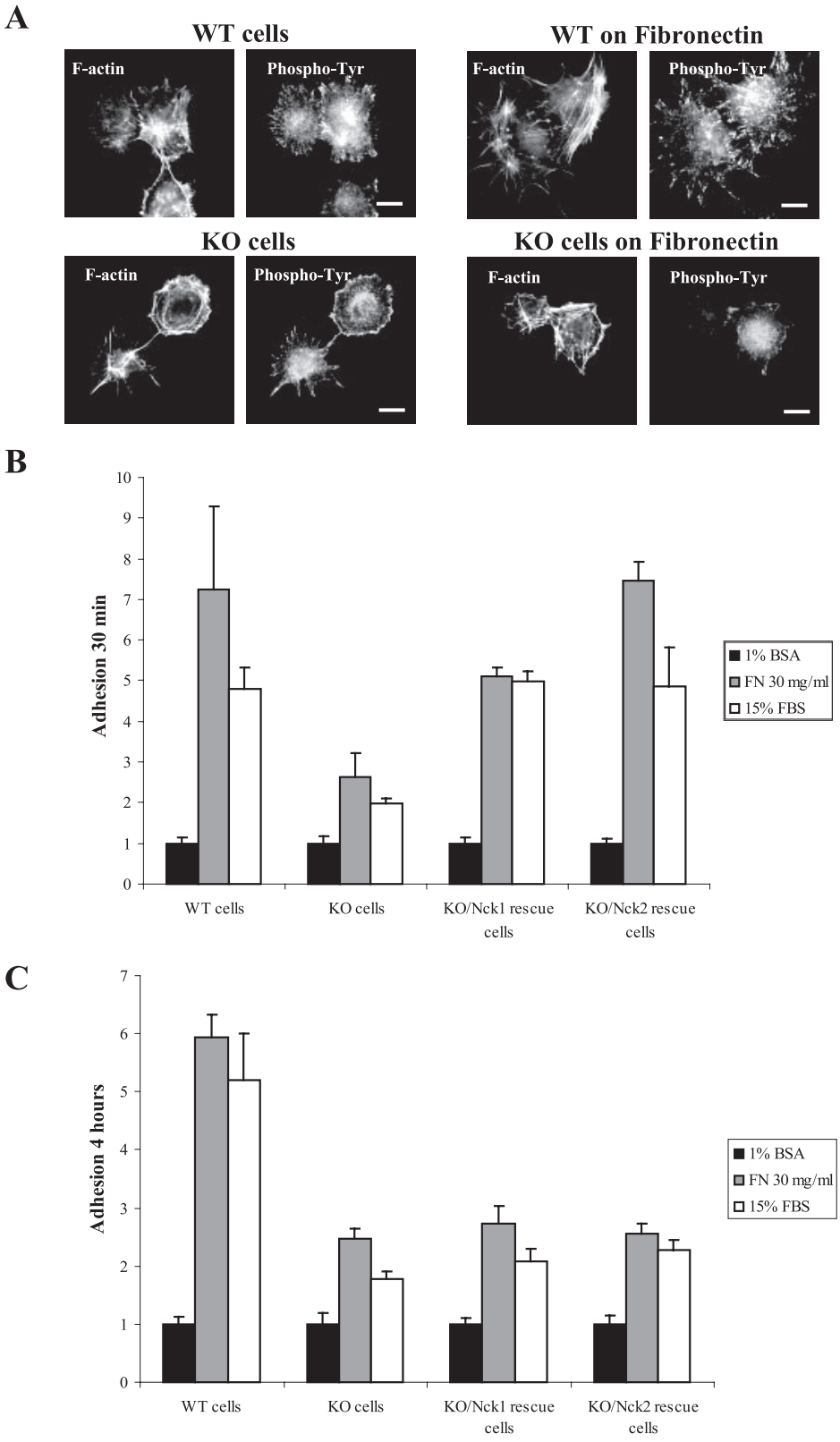

FIGURE 6. **Cells lacking the Nck adapters have a reduced ability to spread on fibronectin.** *A*, WT and KO cells were seeded on untreated glass coverslips or coverslips precoated with fibronectin for 4 h. The cells were fixed, and the focal adhesions were visualized with a mouse monoclonal anti-phosphotyrosine antibody followed by a TRITC-conjugated anti-mouse antibody. Filamentous actin was detected by fluorescein isothiocyanate-conjugated phalloidin. *B*, KO cells were treated as in *A*. The *bar* represents 20 μm. Quantification of the cell adhesion of WT, KO, KO/Nck1 rescue, and KO/Nck2 rescue cells after 30 min (*B*) and 4 h (*C*) is shown. The cells were allowed to attach on microtiter plates counted with 15% FBS, 30 mg/ml fibronectin (*FN*) or 1% bovine serum albumin (*BSA*). The adhesion was expressed as -fold attachment over the values for attachment in 1% bovine serum albumin.

reconstruction of focal adhesions in response to serum treatment.

We next wanted to see if the initial phase of cell attachment was affected by the inability of the KO cells to form focal adhesions. We reasoned that this will affect the adhesive properties of the KO cells compared with the WT counterpart. To test this, cells were plated on glass coverslips that were either uncoated or that had been coated with fibronectin. Cells were fixed 4 h post-seeding, and the focal adhesions were visualized with an antibody against phosphotyrosine. This antibody effectively stains focal adhesions and was used because vinculin was beyond the limit of detection in some of the conditions tested. The WT cells spread on glass with only multiple protrusions, whereas the cells spread on fibronectin formed thicker stress fibers which were associated to the focal adhesions, presumably because the fibronectin-dependent activation of the integrins more efficiently activated the machinery responsible for focal adhesion assembly (Fig. 6*A*). The KO cells attached to the glass and to fibronectin but did not form focal adhesions even when spread on fibronectin (Fig. 6*A*). We also quantified the ability of cells to attach, employing microtiter plates and quantifying cell attachment as described under "Experimental Procedures." The cells were allowed to attach on plates covered with fibronectin or FBS. The difference in adhesive ability between WT and KO cells was apparent when the cells adhered on fibronectin, lending further support for a reduced ability of the KO cells to form focal adhesions (Fig. 6, *B* and *C*). The KO/Nck1 and KO/Nck2 rescue cells had an almost WT ability to adhere under the initial phase, but after 4 h the adhesive properties were close to the KO cells, demonstrating both adapters are required for efficient cell adhesion (Fig. 6, *B* and *C*).

Subcellular Localization of the Components in the Actin Polymerization Machinery Is Altered in KO

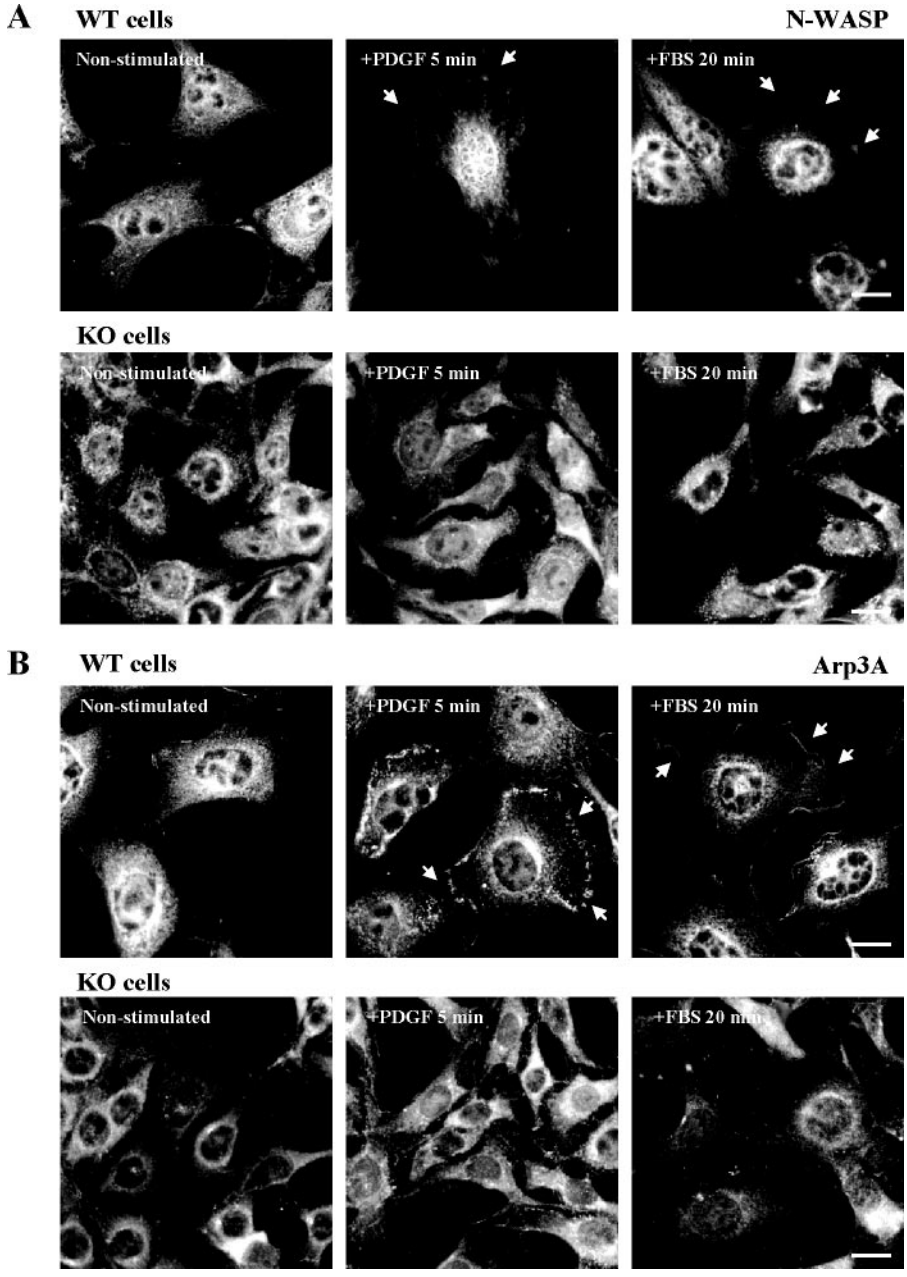

FIGURE 7. **Defects in activation of the actin polymerization machinery in cells lacking NCK adapters.** *A*, localization of endogenous N-WASP in WT and KO cells. The subcellular localization of N-WASP was determined by a rabbit anti-N-WASP antibody followed by a TRITC-conjugated anti-rabbit antibody. *B*, localization of endogenous Arp3A in WT and KO cells. The subcellular localization of Arp3A was determined by a rabbit anti-Arp3A antibody followed by a TRITC-conjugated anti-rabbit antibody. *Arrowheads* show the presence of N-WASP and Arp3A in membrane ruffles. The *bar* represents 20 μm.

Cells—Nck adapters are known to bind key components in the actin polymerization machinery, such as N-WASP. We, therefore, wanted to examine if N-WASP or the Arp2/3 complex is correctly localized in KO cells. Western blot analysis confirmed the presence of N-WASP and Arp3A in the WT and KO cell lines (supplemental Fig. 3*A*). We analyzed the subcellular localization of N-WASP and Arp3A in WT and KO cells. N-WASP localized to dorsal ruffles as well as to edge ruffles in a majority of the WT cells stimulated with PDGF-BB or FBS (Fig. 7*A*). The Arp2/3 component Arp3A also localized to membrane ruffles after stimulation (Fig. 7*B*). The situation in KO cells was different, and we could not detect any localization of neither N-WASP nor Arp3A to the cell margin (Fig. 7, *A* and *B*), suggesting that these proteins are incorrectly localized in cells lacking Nck adapters. The re-expression of Nck1 or Nck2 could not restore the N-WASP relocalization in response to PDGF-BB or FBS (supplemental Fig. 3*B*). In contrast, Arp3A relocalized to the edge ruffles after PDGF-BB stimulation but not serum stimulation in the rescue cell lines, suggesting that either paralogue of Nck can restore the localization of Arp3A to cell areas undergoing membrane ruffling (supplemental Fig. 3*C*).

Activation of Rho GTPases Is Defective in Cells Lacking Nck Adapters—PDGF-dependent signaling is known to lead to activation of the Rho GTPases (24). Therefore, we wanted to examine if the Nck adaptors are involved in the PDGF-BB-stimulated activation of the Rho GTPases Rac1 and RhoA. We stimulated WT and KO cells with PDGF-BB for time periods up to 30 min. The activation of Rac1 was very rapid in the WT cells, and the appearance of GTP-bound Rac1 was already apparent after 2 min of stimulation (Fig. 8*A*). In contrast, PDGF-stimulation did not induce a similar peak of GTP-bound Rac1 in the KO cells (Fig. 8*A*). A similar difference in the activation of Cdc42 was noted; however, the Cdc42 activation was much less prominent compared with the Rac1 activation (data not shown). PDGF stimulation resulted in a slight activation of RhoA in the WT cells; in contrast, PDGF-BB stimulation did not activate RhoA in the KO cells (Fig. 8*A*). We next stimulated WT cells with 10% FBS and recorded a robust activation of RhoA in the WT cells, with a peak after 5 min (Fig. 8*B*). Interestingly, serum stimulation of KO cells resulted in a modest but sustained activation of RhoA (Fig. 8*B*). Taken together, these observations indicate that the signaling to Rho GTPases is dysfunctional in cells lacking Nck adapters.

Because Rac1 and RhoA was not properly activated downstream of the PDGFRβ, we next analyzed if transfection of constitutively active mutants of Cdc42, Rac1, and RhoA could suppress the defects in signaling to the Rho GTPases in cells lacking the Nck adapters. To this end we transient transfected Cdc42/

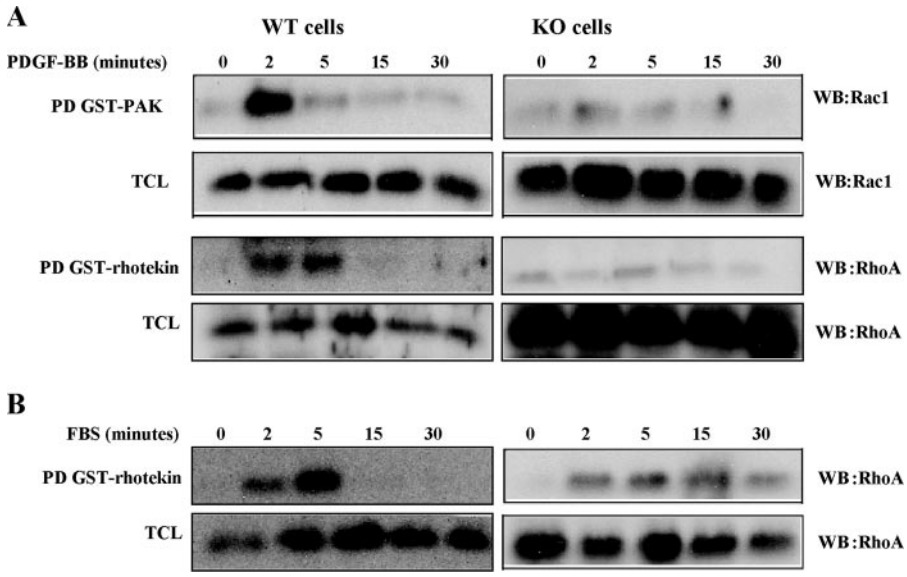

FIGURE 8. **Cells lacking Nck adapters have defective signaling involving Rho GTPases.** *A*, the ability of 100 ng/ml PDGF-BB to activate Rac1 and RhoA was determined in an activation assay. Active, GTP-bound Rac1 and RhoA were detected in GST pulldown assays (*PD*) using the GST-Pak1-CRIB domain and the GST-rhotekin-GBD domain, respectively. The presence of Rac1 or RhoA was detected by Western blotting (*WB*) using the relevant antibodies. *B*, the ability of 10% FBS to RhoA was determined in an activation assay. Active, RhoA was detected in GST pulldown assays using the GST-Rhotekin-GBD domain. The presence of RhoA was detected by Western blotting using the relevant antibodies. *TCL*, total cell lysate.

Q61L, Rac1/Q61L, and RhoA/Q63L into WT and KO cells. Cdc42/Q61L and Rac1/Q61L resulted in a flattening out of the cells associated with a formation of lamellipodia and a concomitant assembly of thin stress fibers, whereas RhoA/Q63L induced a massive bundling of stress-fibers in the WT cells (Fig. 9*A*). This response is in agreement with earlier observations using other fibroblast-like cells (24). In contrast, transfection of Cdc42/Q61L and Rac1/Q61L resulted in different cellular morphology; the cells formed much thicker stress fibers than the one seen in transfected WT cells. This response was associated with an increased rounding up of transfected cells (Fig. 9, *B* and *C*). The rounding up was most pronounced in the KO-expressing RhoA/Q63L cells (Fig. 9, *B* and *C*). This shows that ectopic expression of Rho GTPases cannot fully restore the defects in cell attachment and cytoskeletal dynamics in KO cells, and these cells cannot properly relay the signaling input from the activated Rho GTPases to the downstream events. The prime reason for this is presumably the defects in focal adhesion formation and cell attachment in the KO cells.

DISCUSSION

Nck (now known as Nck1) was originally found in a human melanoma cell library (13). It has been found to possess oncogenic properties based on its ability to induce growth in soft agar and tumors in nude mice (15, 16). The notion that Nck1 is involved in the signaling by tyrosine kinase receptors became established after its identification as a substrate that became phosphorylated upon activation of the PDGFβ receptor (15). Furthermore, it was shown to bind to Tyr-751 in the PDGFβ receptor, which together with Tyr-857 is the major site for tyrosine phosphorylation (7, 25). It has been difficult to study Nck1 alone in this respect, as the Tyr-751 is also a binding site for the p85 subunit of PI3K; however, Tyr-740 actually seems to be the preferred site for p85 (7, 8). This is reflected by our finding that the PDGFRβ/Y751F mutant receptor is still able to activate the phosphorylation of Akt, which is a measure of the activation of PI3K, whereas the PDGFRβ/Y740F mutant receptor could not trigger Akt phosphorylation. This suggests that Tyr-751 predominantly signals via Nck1. Our data suggest that the Nck adapters have more important roles in signaling by the PDGFRβ than acknowledged before. In cells lacking Nck adapters the formation of membrane ruffles, in particular the formation dorsal ruffles after PDGF-BB stimulation, was ablated. The PDGF-induced PI3K-dependent Akt phosphorylation was intact in the KO cells indicating a separation of signaling pathways to Akt and to the actin polymerization machinery downstream of Tyr-751. Dorsal ruffles are thought to constitute a non-clathrin pathway for the sequestration and internalization of tyrosine kinase receptors (26). A similar correlation between Nck and the formation of dorsal ruffles has been observed in another study (27). Interestingly, dorsal ruffles are also missing in cells lacking N-WASP or WAVE1 (28, 29). These observations clearly put Nck and Nck binding partners in a common pathway in the formation of PDGF-induced dorsal ruffles. This is further reflected in the inability of the KO cells to relocalize N-WASP and Arp3A to the cell edges in response to PDGF and serum stimulation.

Several lines of evidence indicate that Nck has an important role in cell migration. This function was first observed in *Drosophila*, where the Nck orthologue Dreadlocks (Dock) was found to be needed for the axon guidance in the fly compound eye (30, 31). Nck is also needed for the actin-based intracellular movement of internalized vaccinia virus particles (32). Observations of PI3K-independent PDGF-induced chemotaxis also suggest that Nck is involved this process (33). Nck is also likely to collaborate with the Crk-associated substrate ($p130^{Cas}$) during PDGF-BB-induced cell migration (27). We noticed that the PDGF-BB-induced chemotactic capacity of the KO cells was reduced to half that of the maximum capacity seen in wild-type cells. Interestingly, serum had a dominant interfering influence on the PDGF induced chemotaxis. We were not able to identify the component in serum responsible for this inhibition. For instance, the common Rho-activating component in serum, lysophosphatidic acid, had no influence on migration of the KO cells (data not shown). Nck, in particular Nck2, has a role in integrin signaling as it binds to PINCH, which in turn binds the integrin-binding tyrosine kinase ILK (34). The absence of Nck2 is likely to result in reduced integrin activation, and we saw a reduction in the number of focal adhesions in the KO cells.

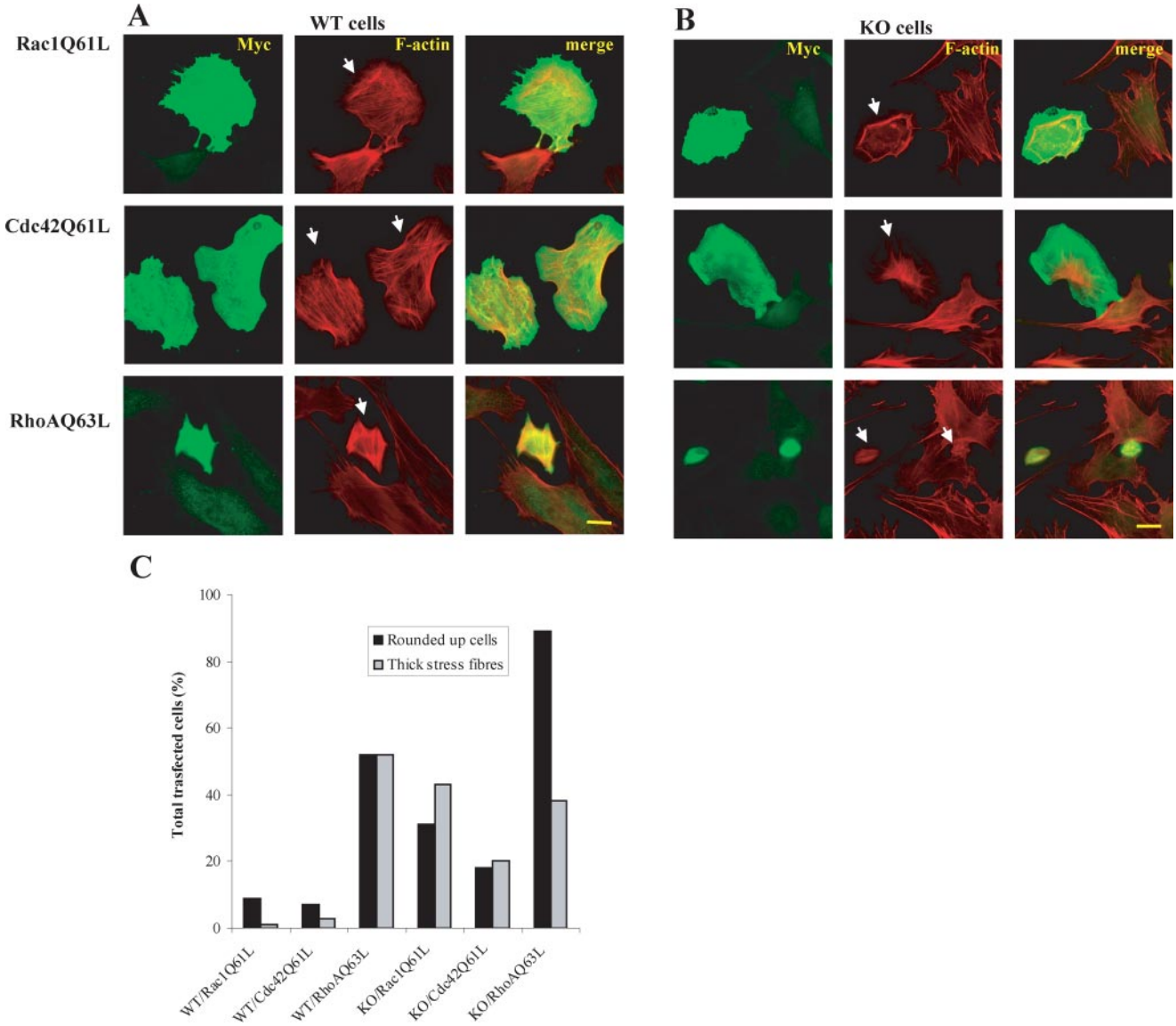

FIGURE 9. **Actin assembly and cell adhesion downstream of the Rho GTPases is altered in cells lacking Nck adapters.** The effect on actin organization by transient transfection of constitutively active mutants of Rho GTPases (Cdc42/Q61L, Rac1/Q61L, and RhoA/Q63L) in WT cells (*A*) or KO cells (*B*). Myc-tagged Rho GTPases were visualized by a Myc-specific mouse antibody followed by an Alexa488-conjugated anti-mouse antibody. Filamentous actin was visualized by TRITC-conjugated phalloidin. The *bar* represents 20 μm. *C*, quantification of the cellular effects induced by the transfection procedure in *A* and *B*. At least 100 transfectants were scored for each condition.

These cells were also less prone to attach and spread during the initial phase after seeding.

Interestingly, the Nck adapters appear to be critical for the activation of the Rho GTPases Cdc42, Rac1, and RhoA downstream of the PDGFRβ. The Rho GTPases are vital for relaying signaling cues from activated cell surface receptors to the actin polymerization machinery (24). Furthermore, the Nck adapters appear to have a role also downstream of the Rho GTPases, in particular downstream of Rac1 and RhoA. We observed that constitutively active mutants of Cdc42 and Rac1 did not induce well organized stress fibers in the KO cells, presumably because the focal adhesions and cell attachment abilities were dysfunctional in these cells. In line with this notion, we noticed a general decrease in the amount of polymerized actin in the KO cells. Targeted localization of Nck to specific foci at the plasma membrane has been shown to lead to a local assembly of the components in the actin polymerization machinery and a local actin polymerization (35). Nck has been shown to mediate *in vitro* actin polymerization together with phosphatidylinositol 4,5-bisphosphate, Rac1, and N-WASP (36). Nck is also implicated in Rac1-mediated actin polymerization as its binding partner, Nap125, forms a multisubunit complex together with PIR121, HSCP300, and WAVE1, which is needed for Rac1-dependent activation of WAVE and the concomitant Arp2/3 dependent actin polymerization (37). Thus, Nck has an important role in mediating the correct subcellular localization of the components of the actin polymerization machinery. It is likely that Nck is required to physically link the activated receptor with the actin polymerization machinery. Interestingly, the epidermal growth factor receptor has been found to bind directly to actin, and actin polymerization appears to form a negative feedback loop as depolymeriza-

tion of the actin filament system by dihydrocytochalasin B leads to enhanced receptor signaling (38, 39). It is possible that actin binding is an element in the regulation of the PDGF receptor function, and Nck could, thus, provide the necessary components of the actin polymerization machinery in close proximity to the PDGF receptor; however, this hypothesis needs further examinations to be fully validated.

REFERENCES

1. Rönnstrand, L., and Heldin, C.-H. (2001) *Int. J. Cancer* **91,** 757–762
2. Tallquist, M., and Kazlaukas, A. (2004) *Cytokine Growth Factor Rev.* **15,** 205–213
3. Wennström, S., Siegbahn, A., Ykote, K., Arvidsson, A. K., Heldin, C.-H., Mori, S., and Claesson-Welsh, L. (1994a) *Oncogene* **9,** 651–660
4. Wennström, S., Hawkins, P., Cooke, F., Hara, K., Yonezawa, K., Kasuga, M., Jackson, T., Claesson-Welsh, L., and Stephens, L. (1994b) *Curr. Biol.* **4,** 385–393
5. Nobes, C. D., Hawkins, P., Stephens, L., and Hall, A. (1995) *J. Cell Sci.* **108,** 225–233
6. Kashishian, A., Kazlauskas, A., and Cooper, J. A. (1992) *EMBO J.* **11,** 1373–1382
7. Nishimura, R., Li, W., Kashishian, A., Mondino, A., Zhou, M., Cooper, J., and Schlessinger, J. (1993) *Mol. Cell. Biol.* **13,** 6889–6896
8. Kazlauskas, A., Kishishian, A., Cooper, J. A., and Valius, M. (1992) *Mol. Cell. Biol.* **12,** 2534–2544
9. Kazlauskas, A., Feng, G.-S., Pawson, T., and Valius, M. (1993) *Proc. Natl. Acad. Sci. U. S. A.* **90,** 6939–6942
10. Rönnstrand, L., Mori, S., Arvidsson, A. K., Eriksson, A., Wernstedt, C., Hellman, U., Claesson-Welsh, L., and Heldin, C. H. (1992) *EMBO J.* **11,** 3911–3919
11. Rönnstrand, L., Arvidsson, A. K., Kallin, A., Rorsman, C., Hellman, U., Engström, U., Wernstedt, C., and Heldin, C.-H. (1999) *Oncogene* **18,** 3696–3702
12. Chen, M., She, H., Kim, A., Woodley, D. T., and Li, W. (2000) *Mol. Cell. Biol.* **20,** 7867–7880
13. Lehmann, J. M, Rietmüller, G., and Johnson, J. P. (1989) *Nucleic Acids Res.* **18,** 1048
14. Braverman, L. E., and Quilliam, L. A. (1999) *J. Biol. Chem.* **274,** 5542–5549
15. Li, W., Hu, P., Skolnik, E. Y., Ullrich, A., and Schlessinger, J. (1992) *Mol. Cell. Biol.* **12,** 5824–5833
16. Chou, M. M., Fajardo, J. E., and Hanafusa, H. (1992) *Mol. Cell. Biol.* **12,** 5834–5842
17. Li, W., Fan, J., and Woodley, D. T. (2001) *Oncogene* **20,** 6403–6417
18. Buday, L., Wunderlich, L., and Tamas, P. (2002) *Cell. Signal.* **14,** 723–731
19. Bladt, F., Aippersbach, E., Gelkop, S., Strasser, G. A., Nash, P., Tafuri, A., Gertler, F. B., and Pawson, T. (2003) *Mol. Cell. Biol.* **23,** 4586–4597
20. Aspenström, P., Fransson, Å., and Saras, J. (2004) *Biochem. J.* **377,** 327–337
21. Demoulin, J. B., Seo, J. K., Ekman, S., Grapengiesser, E., Hellman, U., Ronnstrand, L., and Heldin, C. H. (2003) *Biochem. J.* **376,** 505–510
22. Wennerberg, K., Lohikangas, L., Gullberg, D., Pfaff, M., Johansson, S., and Fässler, R. (1996) *J. Cell Biol.* **132,** 227–238
23. Edlund, S., Landström, M., Heldin, C.-H., and Aspenström, P. (2002) *Mol. Biol. Cell* **13,** 902–914
24. Jaffe, A. B., and Hall, A. (2005) *Annu. Rev. Cell Dev. Biol.* **21,** 247–269
25. Kazlauskas, A., and Cooper, J. A. (1989) *Cell* **58,** 1121–1133
26. Orth, J. D., and McNiven, M. A. (2006) *Cancer Res.* **66,** 11094–11096
27. Rivera, G. M., Antoku, S., Gelkop, S., Shin, N. Y., Hanks, S. K., Pawson, T., and Mayer, B. M. (2006) *Proc. Natl. Acad. Sci. U. S. A.* **103,** 9536–9541
28. Suetsugu, S., Yamazaki, D., Kurisu, S., and Takenawa, T. (2003) *Dev. Cell* **5,** 595–609
29. Legg, J. A., Bompard, G., Dawson, J., Morris, H. L., Andrew, N., Cooper, L., Johnston, S. A., Tramountanis, G., and Machesky, L. M. (2007) *Mol. Biol. Cell* **18,** 678–687
30. Garrity, P. A., Rao, Y., Salecker, I., McGlade, J., Pawson, T., and Zipursky, S. L. (1996) *Cell* **85,** 639–650
31. Rao, Y. (2005) *Int. J. Biol. Sci.* **1,** 80–86
32. Frischknect, F., Moreau, V., Röttger, S., Gonfloni, S., Reckmann, I., Superti-Furga, G., and Way, M. (1999) *Nature* **401,** 926–929
33. Higaki, M., Sakaue, H., Ogawa, W, Kasuga, M., and Shimokado, K. (1996) *J. Biol. Chem.* **271,** 29342–29346
34. Wu, C. (1999) *J. Cell Sci.* **112,** 4485–4489
35. Rivera, G. M., Briceño, C. A., Takeshima, F., Snapper, S. B., and Mayer, B. J. (2004) *Curr. Biol.* **14,** 11–22
36. Rohatgi, R., Nollau, P., Ho, H.-Y. H., Kirscner, M. W., and Mayer, B. M. (2001) *J. Biol. Chem.* **276,** 26448–26452
37. Eden, S., Rohatgi, R., Podtelejnikov, A. V., Mann, M., and Kirschner, M. W. (2002) *Nature* **418,** 790–793
38. den Hartigh, J. C., van Bergen en Henegouwen, P.M.P., Verkleij, A. J., and Boonstra, J. (1992) *J. Cell Biol.* **119,** 349–355
39. Rijken, P. J., van Hal, G. J., van der Heyden, M.A.G., Verkleij, A. J., and Boonstra, J. (1998) *Exp. Cell Res.* **243,** 254–262